Treated oil shale ash and its capacity to remove Cd and Pb from aqueous solutions

Omar Al-Ayed*, Tayel El-Hasan, Abdulaziz Amro, Mohammed Matouq, Fathi Kooli

[a]   Department of Chemical Engineering, Faculty of Engineering Technology, Al-Balqa Applied University, Marka 11134 Amman, Jordan
[b]   Chemistry Department, Mutah University, Al-Karak – 61710, Jordan
[c]   Faculty of Pharmacy, Al-Ahliyya Amman University, Amman, Jordan
[d]   Chemistry Department, Faculty of Science, Islamic University of Madinah, Madinah 42351, Saudi Arabia

Abstract. *Cadmium (Cd) is the most highly toxic heavy metal even at a trace level. In this study, the oil shale ash treated material was used as an adsorbent to remove cadmium and lead (Pb) metals/ions from aqueous solutions. The absorbent treated oil shale material was characterized prior to experimental work using X-Ray Diffraction (XRD) and Scanning Electron Microscopy (SEM). The effects of multiple factors on percent metal removal, including contact time, initial ions concentration and pH, are investigated. Results show that the adsorption capacities of Pb and Cd are 29.15 and 23.81 mgg^{-1}, whereas removal efficiencies are 56% and 48% in 10 minutes, respectively. Removal efficiency and time of equilibrium are affected by the metal atomic weight (Pb 207.2 u and Cd 112.4 u) and pH values. The equilibrium isotherms were analyzed using Freundlich and Langmuir isotherm models and described by the Freundlich isotherm model indicating a heterogeneous surface of the adsorbent. The calculated Langmuir adsorption constant and maximum adsorption capacity of adsorbent, K_L and q_{max}, are $1.313*10^{-2}$ and 25.25, respectively. The Freundlich adsorption constant K_F and the characteristic constant of the Freundlich isotherm n are 0.5234 and 1.39, respectively.*

Keywords: *oil shale ash, lead, cadmium, isotherms, adsorption.*

* Corresponding author: e-mail *omar.alayed@bau.edu.jo*

1. Introduction

Removal of lead (Pb) and cadmium (Cd) from wastewaters emanated from the fact that these elements are harmful to human health. Cadmium is extremely toxic and is classified as carcinogenic, impacting lungs, liver and kidney [1]. Researchers have developed methods to treat wastewater-containing heavy metal ions such as ion exchange [2], oil shale fly ash [3–9] membrane [10], coagulation [11], chemical precipitation [12], adsorption [13], including biosorption, that can remove heavy metals from very dilute aqueous contaminated solutions [14, 15].

However, the most common methods for removing heavy metals are costly, of low efficiency and economically not feasible.

The environment is in collision with heavy metals due to their toxicity and danger to human life if not leached out from waste sources. Heavy metals are transferred to water from a variety of industries, such as wastewater treatment, minerals extraction, metal molding, metal coating processes, batteries manufacturing, nuclear industry, and many others [16]. These heavy metals accumulate in plants (sources of food), and organs of living creatures (consumers), and even in small concentrations would impact the function of life-sustaining cycle [17]. Even a few ppm induces hazardous effects on health such as initiation of cancer, hampering of growth, infection of organs, impairing the nervous system and beneficial microbial communities needed for everyday life functioning [18]. Among the most harmful elements are cadmium, lead, mercury and arsenic [19]; their toxicity and non-biodegradability have a profound impact on the health of our planet.

The burned oil shale ash is considered as a severe environmental problem, because of its friable nature and high enrichment in trace and toxic elements [20–22]. More than two-fold enrichment of trace and toxic elements due to the aerobic combustion process was found in burned oil shale ash by El-Hasan [23]. Extensive research was done with encapsulating toxic elements, particularly Cr, by using natural additives and the aging hydration process [24]. Furthermore, the analytical findings by X-ray absorption near edge structure (XANES), also known as near edge X-ray absorption fine structure (NEXAFS), indicate that the hydration process with increasing time can effectively cause converting the harmful mobile Cr(IV) into the less mobile species Cr(III) form [25].

Oil shale ash and fly ash have been used as cheap sources of leachate or extractive materials of deleterious elements such as cadmium, lead, arsenic, mercury, etc. [20–22]. Oil shale ash adsorbent after activation with sodium hydroxide was tested for Pb and Cd removal from aqueous solutions, the reported absorption capacities were 9 and 12 mg/g, respectively [23]. The alkali-treated oil shale ash from the Huadian power station in China [9] was studied for its ability to extricate lead and cadmium heavy metals from aqueous solutions. The findings of the study showed that the adsorption of lead and cadmium ions by the modified oil shale ash was a function of adsorbent

concentration, pH of the solution, ash particle size and contact time. The modified oil shale ash (oil shale ash fusion by alkali followed by refluxing) was treated with nitric acid, followed by heat treatment at 900 °C to synthesize ZM4 zeolite to remove heavy metals, such as lead, zinc and chromium [24]. The results of removal by ZM4 absorbent were similar to those reported for synthesized fly ash zeolite, ZV4, in which the removal was of the order Pb >Zn > Cr. In the studies by El-Hasan et al. [21, 25], the synthesized zeolitic oil shale ash and fly coal ash by the alkaline fusion hydrothermal method was employed to remove heavy metals such as Pb^{+2}, Cr^{+3}, Cu^{+2}, Cd^{+2} and Zn^{+2} by the ion exchange mechanism. These authors reported an increase in the removal efficiency with increasing dosage and contact time till the equilibrium stage which shows that the synthesized zeolite has a strong affinity for the removal of tested ions. In general, the researchers reported a low capacity of zeolite to leach heavy metals from tested solutions.

The main objective of the current work is to explore the possibility of synthesizing a cheap adsorbent made from treated oil shale ash to adsorb the ions of Pb^{+2} and Cd^{2+} from wastewater. The adsorbents will be subjected to different analyses such as X-Ray Diffraction (XRD), Scanning Electron Microscopy (SEM) and Inductive Coupled Plasma-Mass Spectroscopy (ICP-MS). The study will also investigate the effect of different experimental conditions, time, pH and initial concentrations on adsorption capacity. Furthermore, the equilibrium isotherms will be explored using Langmuir and Freundlich isotherm model equations in addition to kinetic modeling of the adsorption isotherms.

2. Adsorption kinetics development

Adsorption is the physical attachment of molecules, ions, or ions suspended in a liquid, or in a mixture of gases on the surface of a solid adsorbate. The adsorption process is continued and affected by several factors such as adsorbent concentrations, pH of the solution, solid particle size, temperature, and size of adsorbent and contact time till equilibrium is reached.

The adsorption process is normally described through isotherms, i.e. the amount of adsorbate attached to or combined with the adsorbent as a function of concentration is a function of temperature, as indicated by several isotherm equations [26]. Kinetic modeling demonstrates how heavy metals adsorbate ions disperse in the liquid phase to be adsorbed onto the solid phase process till the equilibrium stage is achieved. The empirical formulations of two-parameter isotherms that assume monolayer/multilayer physical adsorption, namely the Langmuir and Freundlich isotherms, have been used to model the removal of heavy metals from aqueous solutions using oil shale ash [27]. Oil shale ash adsorbent was used to remove toxic dyes (crystal violet, methyl orange) from the prepared stock solution [28], in which a pseudo-second-order model was the best fit for the adsorption isotherm curves.

2.1. Langmuir isotherm

The empirical proposed model of the two-parameter Langmuir isotherm for gas-solid physical interaction is employed for different adsorbents [4–6, 28]. The proposed model isotherm that can be written in its linear form which is amenable to linear kinetics analysis is:

$$\frac{C_e}{q_e} = \frac{1}{K_L q_{max}} + \frac{C_e}{q_{max}} ,$$ (1)

where C_e is the concentration of adsorbate metal/ion at equilibrium, mgL^{-1}; q_e is the equilibrium capacity of metal/ions on the surface of adsorbent, mgg^{-1}; q_{max} is the maximum adsorption capacity of adsorbent, mgg^{-1}; and K_L is the Langmuir adsorption constant, Lmg^{-1}. The Langmuir adsorption constants, q_{max} and K_L, are determined from the slope of plotting the Left-Hand Side (LHS) of Equation (1) against the concentration of adsorbate.

2.2. Freundlich isotherm

The Langmuir isotherm assumes a homogeneous adsorbent surface and a monolayer adsorption, whereas the Freundlich isotherm accounts for the heterogeneity of the surface and the multilayer chemisorption adsorption of the adsorbate. The linear equation of the Freundlich isotherm model is expressed as Equation (2):

$$\log(q_e) = \log(K_F) + \frac{\log(C_e)}{n} ,$$ (2)

where the constant K_F is the adsorption constant, mgg^{-1}; n is the characteristic constant of the Freundlich isotherm for the adsorption, taking values between 2 and 10 to indicate good adsorption. To determine the constants of Equation (2), a plot of LHS against $\log(C_e)$ would result in finding the numerical values of the adsorption constant and the characteristic constant from the slope numerical value.

3. Experimental

3.1. Materials and methods

The oil shale sample from El-Lajjun was grounded using a ball mill and pyrolyzed in a tubular furnace at 600 °C for 2 hours under nitrogen inert gas environment.

The ash was prepared after undergoing the pyrolysis process [29], by placing 300 g of the oil shale powder in a cylindrical glass retort and flushing it with nitrogen at a flow rate of 100 ml min^{-1}. During heat-up, the generated

hydrocarbons were passed into a water-cooled receiver. When the desired temperature set point was reached, the heater was switched off immediately, but the N_2 flow was maintained for cooling the retort down to 150 °C. Five ash samples were prepared at temperatures of 600, 650, 700, 750 and 800 °C.

A sample of 10.0 g was activated by 100 ml of 0.1M HCl with shaking for 30 minutes, followed by washing with deionized water. The sample was treated with 100 mL of 0.1M NaOH and shaking for 30 minutes at 120 revolutions per minute (RPM) and 25 °C. The activated sample was washed several times with deionized water and left overnight to dry in an oven at 80 °C.

3.2. Sample characterization

The treated samples were characterized using XRD and SEM.

A 1000 ppm stock solution of Cd and Pb was prepared from the elements' salts, $PbNO_3$ (Panreac) and $Cd(NO_3)_2·4H_2O$ (LOPA Chemie), from which 50 ppm solutions at pH values of 3, 5 and 6 were prepared using 0.1M HCl and 0.1M NaOH for pH adjustment. Samples of 50 mL at several initial concentrations (50, 100, 200, 300 ppm) at pH 5 were also prepared. A quantity of 0.50 g of activated oil shale was immersed in each solution with shaking at 130 RPM and 26 °C. During shaking several samples were withdrawn at 0, 3, 6, 10, 15, 20, 30, 40, 50 and 60 minutes. The samples, each around 0.100 mL, were then diluted to 5.0 mL and analyzed using an Agilent 7700 ICP-MS.

A sample of 0.40 g of activated semi-coke was immersed in 50 mL deionized water in an Erlenmeyer flask and then shaken for 90 minutes at 130 RPM and 26 °C. Water was filtered and analyzed for metals release by ICP-MS.

4. Results and discussion

The studied oil shale sample was subjected to XRD analysis, similar results for Ellajjun oil shale have been earlier obtained by Hamadi et al. [30]. In addition, in the current work, the XRD spectra of activated semi-cokes were measured as shown in Figure 1. As indicated in Figure 1, the intensities of 2θ peaks for calcite ($CaCO_3$), quartz (SiO_2) and apatite ($Ca_5(PO_4)_3(OH,F,Cl)$) increase sharply after pyrolysis and slightly after activation; this is ascribed to the decrease in organic materials content after pyrolysis and the slight loss after activation. The calcite and quartz weight percent contents are estimated to be between 48 and 52%. From Figure 1 it can be seen that the results for calcite, quartz and apatite activated and not activated at different treatment temperatures are almost identical, except for the raw oil shale sample in which the organic part has a limited effect. The removal of hydrocarbon during the pyrolysis process increased the concentration of quartz, calcite and apatite due to the loss of the hydrocarbon fraction. This resulted in more prominent peaks of other nonhydrocarbon compounds.
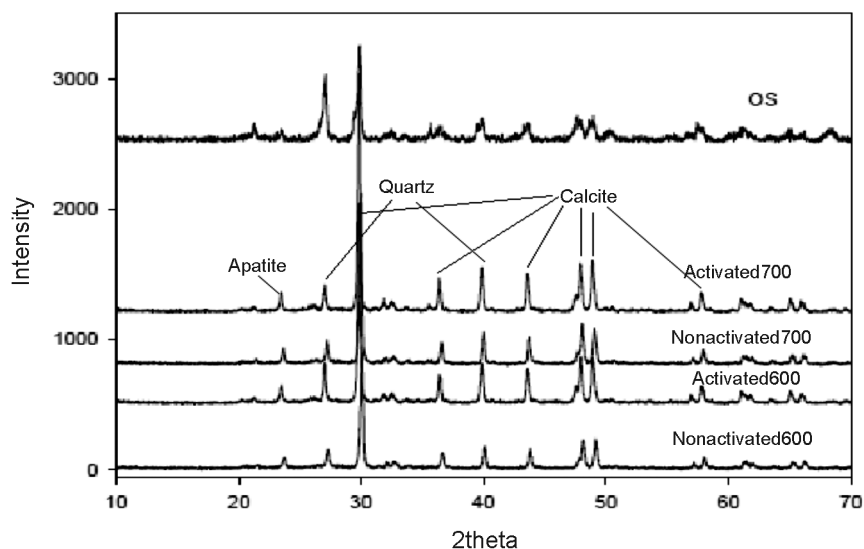
Fig. 1. XRD spectra for activated and nonactivated oil shale.

4.1. Scanning Electron Microscopy

The scanning electron microscope images (Quantum 200 unit) give a clear picture of the oil shale's physical structure and porosity (Fig. 2). The scanning electron micrographs of the activated semi-coke at different magnifications, 1000x and 10000x, present quartz and calcite as major constituents of the studied sample. It is quite obvious from these scans that the structure of the oil shale ash is very porous and has voids of different sizes.

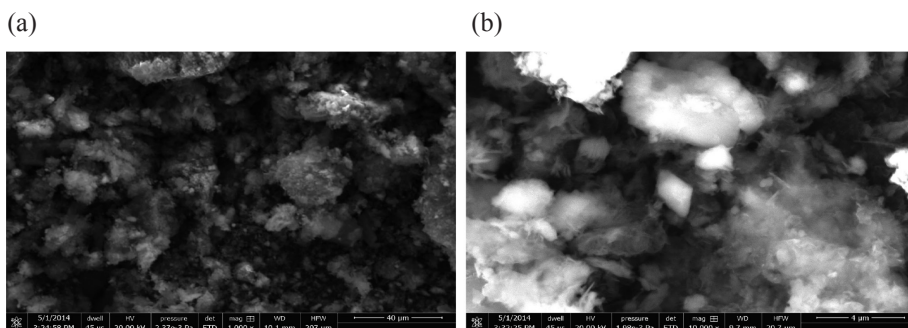(a)   (b)

Fig. 2. Scanning electron microscope images of oil shale at different magnifications: a) activated semi-coke, 1000x; b) activated semi-coke, 10000x.

4.2. Metal removal study

4.2.1. Metal solution pH

The influence of solution pH on metal adsorption is well known since it affects the nature and chemistry of heavy metals during the adsorption process [31–35]. The effect of pH on the adsorption of metal was tested and the results obtained are depicted in Figure 3. As can be seen from the figure, pH of 3, 5 and 6 were used in this work. The results are depicted as the percent of Pb and Cd metals/ions removal through adsorption onto 0.50 g of semi-coke as a function of time. Figure 3 also shows that the percent removal of Pb and Cd ions at a selected period of 6 minutes and pH of 5 is 55% and 21%, respectively, whereas at pH of 3 it is 40% and 47%, respectively, and at pH of 6, respectively 28% and 23%. With pH decreasing from 5 to 3, the percent removal of Pb decreased to 49%, whereas that of Cd increased from 21% to 47%. In other words, at 6 minutes of adsorption, for Pb, pH5>pH>3>pH6, whereas during the adsorption for Cd the pH changes as follows: pH6>pH3>pH5. This gives evidence of that the type and size of metal ions are as important as is the pH value. Since the size of a Cd ion is much smaller than that of Pb, the absorption of Cd reached a constant percent removal in shorter time than the same process with Pb. It is clear from Figure 3 that the percent removal of Cd continuously increased with time at pH of 3 till the end of the run, unlike the Pb percent removal which reached almost a fixed value of 48% at about 20 minutes of the run. This demonstrates that the adsorption is also affected by the available pore size distribution of the activated semi-coke. On the other hand, the maximum percent removal achieved at pH of 3, 5 and 6 is 55%, 58% and 48% for Pb and 42%, 54% and 53% for Cd, respectively. It is evident that a pH value of 5 results in the higher removal efficiency and a shorter time to achieve maximum removal compared with the other values of pH.
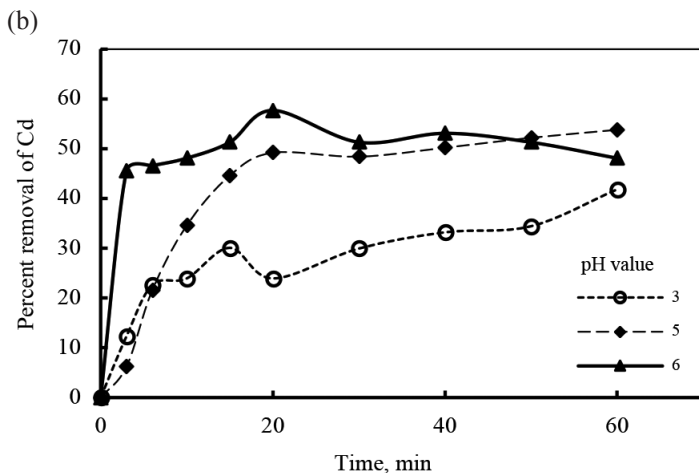
(a)

(b)
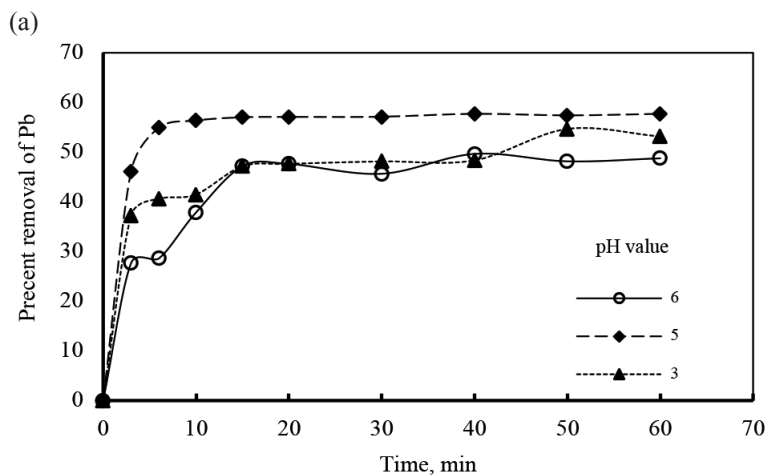
Fig. 3. The effect of solution pH on the adsorption of Pb and Cd at 0.5 g oil shale ash loading: a) Pb; b) Cd.

4.2.2. Effect of initial metal concentration

The effect of the initial concentrations of Pb and Cd metals on their removal onto 0.5 g of oil ash is depicted in Figure 4. Solutions of 300, 200 and 100 ppm are prepared as indicated in section 2.2. The obtained results as percent removal of metal as a function of time at pH of 5 are plotted in Figure 4. The figure displays that after a 10-minute adsorption, the percentage of removal is 47%, 39%, 64% and 60% for Pb, and 29%, 29%, 42% and 48% for Cd at 300, 200, 100 and 50 ppm loadings, respectively. The lower the loading of the metals/ions, the higher their percent removal. Similarly, the removal percentage of smaller-sized Cd ions increased with time compared with larger-sized Pb ions and reached a final value in shorter time. The maximum percent removal of larger Pb ions is higher than that of smaller Cd ions.
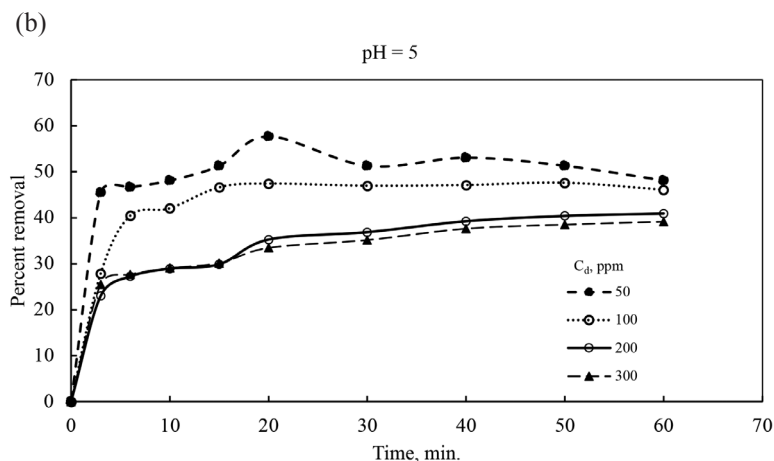
(a)

(b)
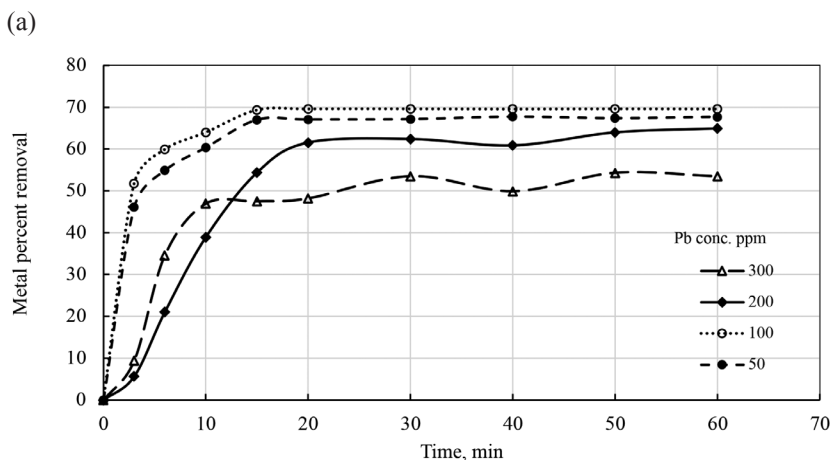
Fig. 4. The percent removal of Pb and Cd at pH of 5 and different metal concentrations by 0.5 g of activated semi-coke: a) Pb; b) Cd.

Figure 4 also shows that the removal efficiency of Pb of the 300 ppm initial concentration increased from 48% at 10 minutes to 53% in 30 minutes and then fluctuated around 53% till 60 minutes of the run which gives evidence of saturation of the oil shale semi-coke adsorption capacity. A similar behavior is observed for Cd with lower percent removal efficiencies. On the other hand, the initial removal of the Pb metal of the 200 ml initial concentration is slower than that of the 300 ppm Pb but with higher efficiency, reaching 62% in 20 minutes and for longer times till the end of the run. Figure 4 exhibits that the percent removal of Cd of the 200 ppm initial concentration is similar to that of the element with the initial concentration of 300 ppm. Contrary to these results, the 100 and 50 ppm initial concentrations have shown a similar behavior for the Pb metal/ion, but slightly different for the Cd metal, in the case of which the 50 ppm concentration displayed a higher percent removal than the 100 ppm initial concentration. These two concentrations, 100 and 50 ppm, have demonstrated a very fast removal process at the initial time, in less than 6 minutes, reaching the maximum removal efficiency of 68% at about 15 minutes of the run time. It is worth noting that the semi-coke was saturated in 15–20 minutes.

The results in Figure 4 can be further used to explore the mass of metal removed by oil shale semi-coke from solution. The maximum mass amount removed from the initial loading of solution at 15 minutes is displayed in Figure 5. In this figure, the total mass removed converted from the calculated efficiency is plotted against the total loadings of the solution at pH of 5.
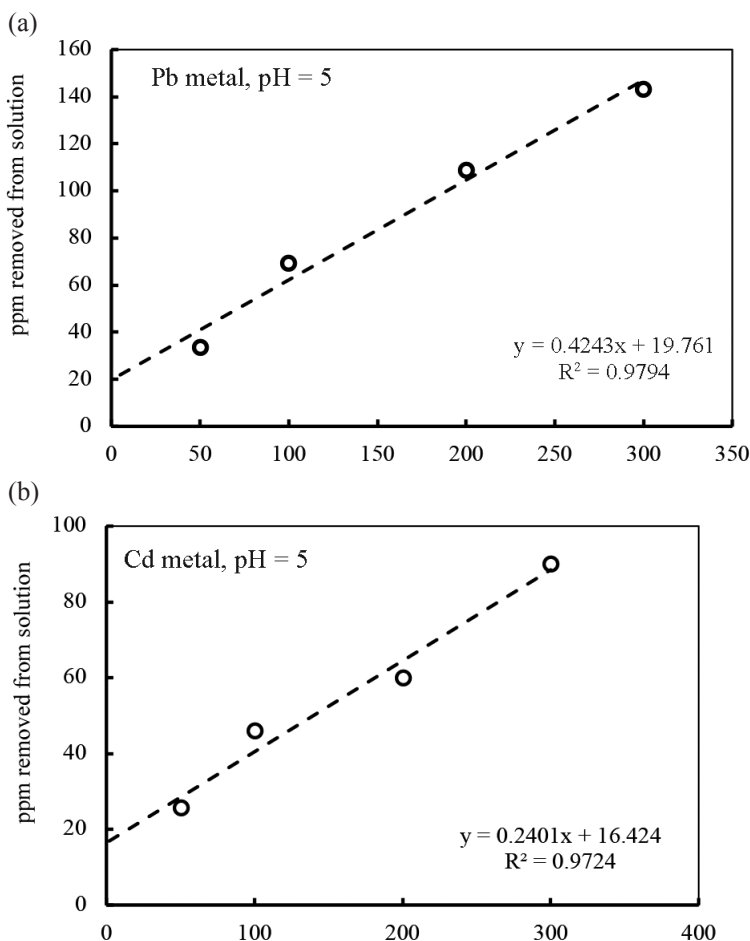
(a)

(b)

Fig. 5. The mass of metals removed at different metal loadings of solution and pH of 5: a) solution content of Pb metal, ppm; b) solution content of Cg metal, ppm.

It is clear from Figure 5 that the mass removed from solution is directly proportional to the metal loading. The linear relationship between the mass removed and the metal loading can be represented by the linear equation displayed in Figure 5, with R^2 being 0.972. From the figure it can be observed that the slope of the Pb curve is almost double that of Cd, indicating the higher mass removal from the original solution for Pb than for Cd metals/ions.

5. Adsorption isotherms

The adsorption isotherms curves that describe interactions between the adsorbate molecules and the active sites on the solid surface of the adsorbent are the dynamic representation of these interactions. There are two types of adsorption isotherms most frequently used by researchers. The Langmuir and Freundlich adsorption isotherm models were employed to analyze the experimental data [5, 28]. The Langmuir isotherm model, Equation (1), is the most widely used equation for modeling equilibrium data in solid-liquid adsorption systems. This model was valid for only the monolayer adsorption onto the adsorbent surface. The linear form of the Langmuir equation which is used to plot data and estimate the constants was represented by Equation (1).

5.1. Langmuir isotherm

Equation (1) is employed for the analysis and determination of constants. Plotting the experimental results to determine q_{max}, the maximum adsorption capacity of adsorbent (mgg^{-1}) and K_L, the Langmuir adsorption constant (Lmg^{-1}) was related to the affinity of the adsorption site. As can be seen from Figure 6, the data are falling in a straight line in which the calculated values of q_{max} and K_L are 25.25 and $1.313*10^{-2}$, respectively, with the linear regression coefficient R^2 being 0.9855. The low adsorption constant value gives evidence of weak interactions between the adsorbate and the adsorbent material.

It is obvious from Figure 6 that the experimental data are fitted to a straight line, which is in agreement with the linear form of the Langmuir equation (1).
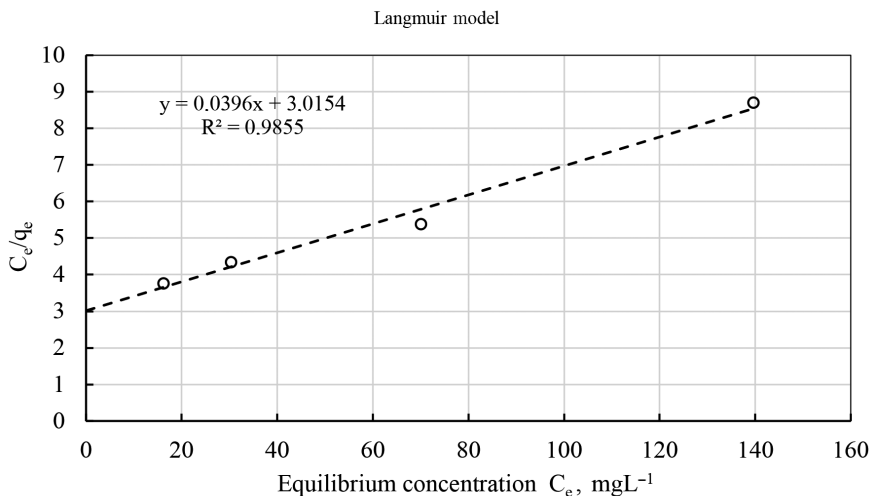

Fig. 6. The determination of Langmuir isotherm model constants.

5.2. Freundlich isotherm

The Langmuir model assumes the homogeneity of the surface and has an equal probability for the adsorption of a monolayer of the adsorbate. The Freundlich model is different from the assumption of the Langmuir model in which it represents a multilayer and heterogeneous surface adsorption mechanism. Equation (2) is a linear form of the Freundlich isotherm in which a plot of $\log(q_e)$ vs the quantity $\log(C_e)$ will culminate in the determination of K_F and n from the intercept and slope of the plot. Figure 7 shows fitting experimental data to Equation (2).

Freundlich model
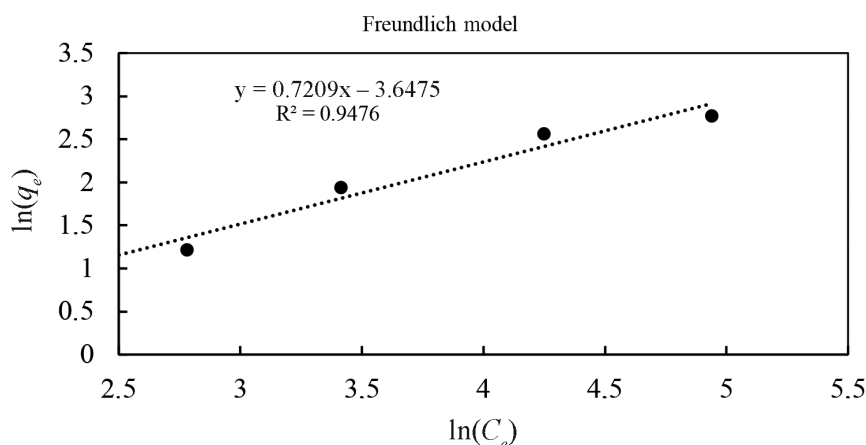
$$y = 0.7209x - 3.6475$$
$$R^2 = 0.9476$$

Fig. 7. The determination of Freundlich isotherm model constants.

The values of the constants K_F and n of Equation (2) are estimated from the plot of Figure 7. The K_F ($mg^{1-(1/n)} L^{1/n} \cdot g^{-1}$) and n are Freundlich constants that characterize adsorption capacity and binding capacity, respectively. The values of the adsorption capacity constant K_F and the binding capacity are found to be 0.5234 and 1.39, respectively, with the value of the regression constant R^2 being 0.9476.

For the Langmuir isotherm the calculated value of the constant K_L is $1.313*10^{-2}$, whereas for the Freundlich isotherm, the calculated value of the constant K_F is 0.5234, which is almost 40 times higher than that of K_L, indicating a strong multilayer adsorption of the adsorbent. This result favors the Freundlich isotherm model to represent the adsorption process of this work.

6. Removal of Pb and Cd metals/ions from water using treated oil shale

A mixture of lead and cadmium at pH of 5 was subjected to absorption using treated oil shale ash. To investigate the preference for simultaneous absorption of both Pb and Cd onto the surface of the semi-coke, an experiment was conducted. A mixture containing 100 ppm of both Pb and Cd was prepared and subjected to absorption with activated oil shale semi-coke. The absorption results are shown in Figure 8. The percent removal of Pb and Cd is presented as a function of time. From Figure 8 it can be seen that initially, the removal percent is higher for Cd till about 10 minutes' time onstream at which its absorption reached almost saturation. After the 10-minute absorption, the rate of Pb removal increases with increasing time as shown in Figure 8. The maximum removal of Cd is 35%, whereas the maximum removal of Pb kept increasing with time, reaching 50% at the end of the run.
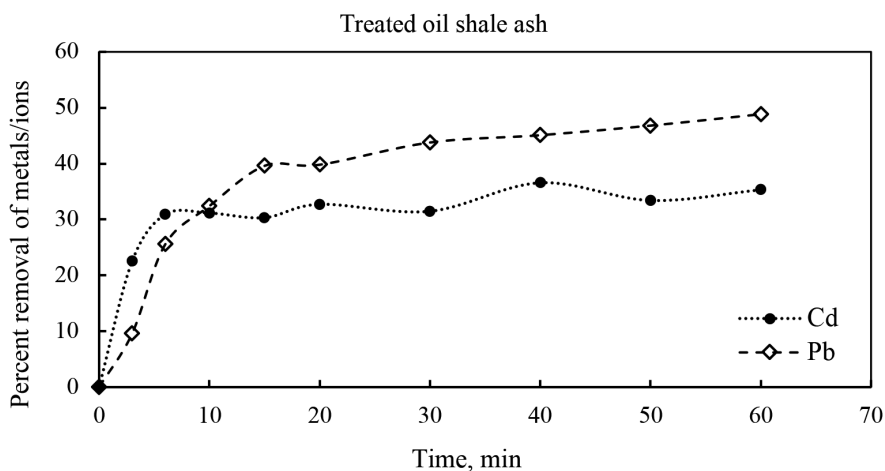
Fig. 8. Absorption of Pb and Cd onto treated oil shale ash, at pH 5.

7. Metals/ions release study

An experiment was carried out to determine the content of different metals/ions in oil shale semi-coke and their release (desorption) from oil shale ash to water. The 0.4 g mass of oil shale semi-coke after pyrolyzing at 600 °C was immersed in 50 mL deionized water in an Erlenmeyer flask and then shaken for 90 minutes at 130 RPM and 26 °C. Prior to metals release, water was filtered and analyzed using an Agilent 7700 ICP-MS.

The results of ICP-MS are presented in Table, the concentrations of the metals detected in oil shale ash are given in ppb. It is clear from Table that

there was no release of metals/ions from oil shale semi-coke to water. This indicates that no metals/ions are released from oil shale semi-coke during the adsorption of metals, especially Pb and Cd, from solution to oil shale ash.

Table. Metals/ions released from oil shale ash to solution

Metal	Oil shale ash at 600 °C, ppb	Oil shale ash at 700 °C, ppb
Cd	≤ 0.06	≤ 0.06
Pb	≤ 0.09	≤ 0.09
Cr	≤ 0.07	≤ 0.07
Fe	≤ 0.07	≤ 0.07
Co	≤ 0.01	≤ 0.01
Ni	≤ 0.01	≤ 0.01
Cu	≤ 0.06	≤ 0.06
Zn	2.1	2.2
As	≤ 0.01	≤ 0.01

8. Conclusions

In this research work, treated oil shale semi-coke has been utilized as an adsorbent to remove lead and cadmium metals/ions from aqueous solutions. The X-ray diffraction of oil shale and semi-coke showed the peak release for calcite, apatite and quartz. Scanning electron microscopy indicated a high surface area and clear images of calcite. The contact time demonstrated that adsorption equilibrium was achieved after 10–15 minutes, furthermore, the higher pH values of metals/ions solution gave evidence of their higher removal. According to isothermal study, the metals/ions adsorption was represented by the Freundlich model describing a heterogeneous multilayer adsorption. The activated oil shale semi-coke did not release any metals/ions from the solid phase to solution. The Langmuir isotherm was found to better fit the results, indicating a monolayer adsorption.

Acknowledgements

REFERENCES

1. Pyrzynska, K. Removal of cadmium from wastewaters with low-cost adsorbent. *J. Environ. Chem. Eng.,* 2019, **7**(1**)**, 102795.
2. Al-Enezi, G., Hamoda, M. F., Fawzi, N. Ion exchange extraction of heavy metals from wastewater sludges. *J. Environ. Sci. Health A*, 2004, **39**(2), 455–464.
3. Shawabkeh, R., Al-Harahsheh, A., Hami, M., Khlaifat, A. Conversion of oil shale ash into zeolite for cadmium and lead removal from wastewater. *Fuel*, 2004, **83**(**7**–8), 981–985. doi.org/10.1016/j.fuel.2003.10.009
4. Bai, S., Chu, M., Zhou, L., Chang, Z., Zhang, C., Guo, H., Liu, B., Wang, S. Modified oil shale ash and oil shale ash zeolite for the removal of Cd^{2+} ion from aqueous solutions. *Environ. Technol.*, 2019, **40**(11), 1485–1493. doi.org/10.1080 /09593330.2018.1537311
5. Zhu, B. L., Xiu, Z. M., Liu, N., Bi, H. T., Lv, C. X. Adsorption of lead and cadmium ions from aqueous solutions by modified oil shale ash. *Oil Shale*, 2012, **29**(3), 268–278.
6. Flores, R., Espinoza, S. Kinetics studies on the process of Zn removal from wastewater using ultrasonically activated sorbents. *Chem. Biochem. Eng. Q.*, 2017, **31**(1), 123–130.
7. Pimentel, P. M., Oliveira, R. M. P. B., Melo, D. M. A., Melo, M. A. F., Assunção, A. L. C., Gonzales, G. Adsorption of chromium ions on oil shale waste. *Braz. J. Pet. Gas*, 2011, **5**(2), 65–73.
8. Bao, W., Liu, L., Zou, H., Gan, S., Xu, X., Ji, G., Gao, G., Zheng, K. Removal of Cu^{2+} from aqueous solutions using Na-A zeolite from oil shale ash. *Chinese J. Chem. Eng.*, 2013, **21**(9), 974–982.
9. Lees, H., Järvik, O., Konist, A., Siirde, A., Maaten, B. Comparison of the ecotoxic properties of oil shale industry by-products to those of coal ash. *Oil Shale*, 2022, **39**(1), 1–19.
10. Ghasem, N., Al-Marzouqi, M., Abdul Rahim, N. Removal of cadmium from industrial wastewater using water-soluble polymer via hollow fiber membranes. *Int. J. Petrochem. Sci. Eng.*, 2016, **1**(4), 88–90. DOI: 10.15406/ ipcse.2016.01.00016
11. Un, U. T., Ocal, S. E. Removal of heavy metals (Cd, Cu, Ni) by electrocoagulation. *Int. J. Environ. Sci. Dev.*, 2015, **6**(6), 425–429. DOI: 10.7763/IJESD.2015.V6.630
12. Parmar, K. Removal of cadmium from aqueous solution using cobalt-silicate-precipitation tube (CoSPT) as adsorbent. *Int. J. Sci. Inventions Today*, 2013, **2**(3), 204–215.

13. He, S., Li, Y., Weng, L., Wang, J., He, J., Liu, Y., Zhang, K., Wu, Q., Zhang, Y., Zhang, Z. Competitive adsorption of Cd^{2+}, Pb^{2+} and Ni^{2+} onto Fe^{3+}-modified argillaceous limestone: influence of pH, ionic strength, and natural organic matters. *Sci. Total Environ.*, 2018, **637–638**, 69–78.

14. Beni, A. A., Esmaeili, A. Biosorption, an efficient method for removing heavy metals from industrial effluents: A Review. *Environ. Technol. Innov.*, 2020, **17,** 100503.

15. Matouq, M., Saleh, M., Al-Ayed, O., El-Hasan, T., Hiroshi, Y., Tagawa, T. Biosorption of chromium and nickel from aqueous solution using pine cones, eucalyptus bark, and moringa pods: a comparative study. *Water Pract. Technol.*, 2021, **16**(1), 72–82.

16. Genevois, N., Villandier, N., Chaleix, V., Poli, E., Jauberty, L., Gloaguen, V. Removal of cesium ion from contaminated water: Improvement of Douglas fir bark biosorption by a combination of nickel hexacyanoferrate impregnation and TEMPO oxidation. *Ecol. Eng.*, 2017, **100**, 186–193.

17. Huang, Y., Chen, Q., Deng, M., Japenga, J., Li, T., Yang, X., He, Z. Heavy metal pollution and health risk assessment of agricultural soils in a typical peri-urban area in southeast China. *J. Environ. Manage.*, 2018, **207**, 159–168.

18. Çolak, F., Atar, N., Yazıcıoğlu, D., Olgun, A. Biosorption of lead from aqueous solutions by *Bacillus* strains possessing heavy-metal resistance. *Chem. Eng. J.*, 2011, **173**(2), 422–428.

19. Jyothi, N. R. Heavy metal sources and their effects on human health. In: *Heavy Metals: Their Environmental Impacts and Mitigation* (Nazal, M., Zhao, H., eds,). IntechOpen, London, 2020. DOI: 10.5772/intechopen.95370

20. El-Hasan, T. Geochemistry of redox-sensitive trace elements and its implication on the mode of formation of the Upper Cretaceous oil shale, Central Jordan. *Neues Jahrb. Geol. Palaontol. Abh.*, 2008, **249**(3), 333–344.

21. El-Hasan, T., Szczerba, W., Buzanich, G., Radtke, M., Riesemeier, H., Kersten, M. Cr(VI)/Cr(III) and As(V)/As(III) ratio assessments in Jordanian spent oil shale produced by aerobic combustion and anaerobic pyrolysis. *Environ. Sci. Technol.*, 2011, **45**(22), 9799–9805.

22. El-Hasan, T., Mahasneh, B. Z., Abdel Hadi, N., Abdelhadi, M. High calcium ash incorporating into clay, sand and cement mortars used for encapsulation of some heavy metals. *Jordan Journal of Earth and Environmental Sciences (JJEES)*, 2014, **6**(3), 23–28.

23. El-Hasan, T. Characteristics and environmental risks of the oil shale ashes produced by aerobic combustion and anaerobic pyrolysis processes. *Oil Shale*, 2018, **35**(1), 70–83.

24. El-Hasan, T., Abu-Jaber, N., Abdelhadi, N. Hazardous toxic elements mobility in burned oil shale ash, and attempts to attain short- and long-term solidification. *Oil Shale*, 2019, **36**(2S), 226–249.

25. El-Hasan, T., Harfouche, M., Aldrabee, A., Abdelhadi, N., Abu-Jaber, N., Aquilanti, G. Synchrotron XANES and EXAFS evidence for Cr^{+6} and V^{+5} reduction within the oil shale ashes through mixing with natural additives and

hydration process. *Heliyon,* **7**(4), e06769. https://doi.org/10.1016/j.heliyon.2021. e06769

26. Kuusik, R., Uibu, M., Kirsimäe, K. Characterization of oil shale ashes formed at industrial-scale CFBC boilers. *Oil Shale*, 2005, **22**(4S), 407–419.

27. Bai, S., Chu, M., Zhou, L., Chang, Z., Zhang, C., Liu, B. Removal of heavy metals from aqueous solutions by X-type zeolite prepared from combination of oil shale ash and coal fly ash. *Energ. Source. Part A*, 2022, **44**(2), 5113–5123. DOI: 10.1080/15567036.2019.1661549

28. Al-Harahsheh, M., Al-Ayed, O., Robinson, J., Kingman, S., Al-Harahsheh, A., Tarawneh, Kh., Saeid, A., Barranco, R. Effect of demineralization and heating rate on the pyrolysis kinetics of Jordanian oil shales. *Fuel Process. Technol.*, 2011, **92**(9), 1805–1811.

29. Zhao, Z., Yuan, J., Fu, M., Su, L., Li, Z. Removal of methylene blue from aqueous solution by using oil shale ash. *Oil Shale*, 2014, **31**(2), 161–173.

30. Hamadi, A., Nabih, K. Synthesis of zeolites materials using fly ash and oil shale ash and their applications in removing heavy metals from aqueous solutions. *J. Chem*., 2018, **3**, ID 6207910, doi.org/10.1155/2018/6207910

31. Bai, S., Zhou, L., Chang, X., Zhang, C., Chu, M. Synthesis of Na-X zeolite from Longkou oil shale ash by alkaline fusion hydrothermal method. *Carbon Resour. Convers*., 2018, **1**(3), 245–250.

32. Foo, K. Y., Hameed, B. H. Insights into the modeling of adsorption isotherm systems. *Chem. Eng. J.*, 2010, **156**(1), 2–10.

33. Bao, W. W., Zou, H. F., Gan, S. C., Xu, X. C., Ji, G. J., Zheng, K. Y. Adsorption of heavy metal ions from aqueous solutions by zeolite based on oil shale ash: Kinetic and equilibrium studies. *Chem. Res. Chin. Univ.*, 2013, **29**(1), 126–131.

34. Miyah, Y., Benjelloun, M., Lahrichi, A., Mejbar, F., Iaich, S., El Mouhri, G., Kachkoul, R., Zerrouq, F. Highly-efficient treated oil shale ash adsorbent for toxic dyes removal: Kinetics, isotherms, regeneration, cost analysis and optimization by experimental design. *J. of Enviro. Chem. Eng*., 2021, **9**(6), 106694.

35. Neshumayev, D., Pihu, T., Siirde, A., Järvik, O., Konist, A. Solid heat carrier oil shale retorting technology with integrated CFB technology. *Oil Shale*, 2019, **36**(2S), 99–113.